

# Cycle-by-Cycle Queue Length Estimation for Signalized Intersections Using Sampled Trajectory Data

Yang Cheng, Xiao Qin, Jing Jin, Bin Ran, and Jason Anderson

**Queue length estimation is an important component of intersection performance measurement. Different approaches based on different data sources have been presented. With the latest developments in vehicle detection technologies, especially probe vehicle technologies, use of vehicle trajectory data has become possible. In this paper, an improved method for queue length estimation for signalized intersections is proposed. This method is able to provide cycle-by-cycle queue length estimation for signalized intersections with sampled vehicle trajectories as the only input. The keystone of the entire approach is the concept of the critical point (CP), which represents the changing vehicle dynamics. A CP extraction algorithm is introduced to identify CPs from raw trajectories. Using the CPs related to queue formation and dissipation, the authors propose an improved queue length estimation method based on shock waves. The performance of this approach is evaluated with several data sets under different flow and signal timing scenarios, including a recently collected data set from a Global Positioning System logger. The results indicate that this trajectory-based approach is promising.**

Queue length is one of the most important performance measures of an intersection. Through the use of queue length, other arterial performance measures, such as intersection delay, travel time, and level of service can be estimated quite readily. For traffic engineers, these performance measures provide indicators for identifying problems, thereby helping decision makers improve the level of service from individual intersections to the entire road network (1). The provision of timely and accurate performance measures to travelers can save travel time and costs.

The problem of queue length estimation has been investigated for about five decades. Many approaches based on different data sources have been presented. In general, on the basis of the problem formulation, most queue length estimation methods can be classified in two categories: input–output models (2–5) and shock wave models (6–9). Input–output models can be generalized as the analysis of vehicle accumulation before the intersection. Most early mod-

els are steady-state models, in which traffic demands are assumed to be constant and the input and output flows reach equilibrium (2, 10). Further improvement includes providing queue length in small time stamps on the basis of vehicle arrival and departure profiles, first applied in the software TRANSYT (11). This approach was later extended and named the incremental queue accumulation method (12, 13). Stochastic analysis is also introduced to address the stochastic and dynamic nature of arterial traffic (10, 14). Several recent studies formulate traffic queuing as a Markov chain renewal process (15–18); the queue length is thus estimated on the basis of the condition of previous time steps. The other category of models is based on shock waves of the queue formation and dissipation. These shock wave models can provide detailed temporal and spatial information for the queuing process (6, 7, 19).

Queue length estimation methods leading to practical applications are limited. One of the major difficulties that input–output models encounter is the occurrence of long queues. When the rear of the queue exceeds the advance vehicle detector that provides the arrival traffic volume, the inflow cannot be accurately obtained; the result is large estimation errors (8, 9). This limitation is significant because long queues are common on congested arterial links. Although analysis based on shock waves is able to address the problem of long queues (9), detailed information about traffic conditions is required to detect the necessary shock waves; this information is difficult to obtain through existing arterial traffic data collection systems.

Recent studies indicate an increasing interest in providing real-time estimates of queue length (3, 9, 20, 21). These studies show the benefit and importance of using new data sources, such as high-resolution loop detector data (aggregated in small time intervals or individual vehicle counts) and probe vehicle data. As a new format of probe data, vehicle trajectory data is a topic attracting researchers' interest. Several studies use trajectory data for shock wave detection (22, 23), whereas a few focus on intersection performance. Comert and Cetin (24) studied the conditional probability distribution of the queue length at an isolated intersection given the locations of probe vehicles in the queue. They found that only the location of the last probe in the queue is necessary for queue length estimation. However, the assumption that the actual percentage of probe vehicles among the traffic stream is known limits the application of this method. A simulation study by Shladover and Kuhn (25) investigated the feasibility of using probe trajectories, but it also follows the sampled travel time approach. An impressive study about free-way travel time estimation was conducted by Claudel et al. (26), in which the probe trajectory measurement was converted to density estimation using the Moskowitz function (27, 28).

Using probe trajectory data for arterial performance measurement is more complicated because of the periodic turbulence from signals

---

Y. Cheng and J. Jin, Department of Civil and Environmental Engineering, University of Wisconsin–Madison, 2205 Engineering Hall, 1415 Engineering Drive, Madison, WI 53706-1691. X. Qin and J. Anderson, Civil and Environmental Engineering, South Dakota State University, Crothers Engineering Hall 120, 2219, Brookings, SD 57007. B. Ran, Department of Civil and Environmental Engineering, University of Wisconsin–Madison, Madison, WI 53706 and School of Transportation, Southeast University, No. 2 Si Pai Lou, Nanjing 210096, China. Corresponding author: Y. Cheng, cheng8@wisc.edu.

*Transportation Research Record: Journal of the Transportation Research Board*, No. 2257, Transportation Research Board of the National Academies, Washington, D.C., 2011, pp. 87–94.  
DOI: 10.3141/2257-10

and local frictions. A primary shock wave-based model using the vehicle trajectory data has been demonstrated in the authors' previous work (29). An improved approach is presented in this paper. This approach is tested by numeric experiments using simulation data, real trajectory data from the next generation simulation program (NGSIM) (30), and Global Positioning System (GPS) data from recently collected field data. The paper concludes with an overview of the study and a discussion of future work.

**METHODOLOGY**

Given the intersection and link geometric characteristics, the intent is to develop a real-time estimation model for intersection queue length using vehicle trajectory data as the only input. The trajectory of a vehicle can be represented as a series of points,  $\{x_t\}$ , where  $x_t$  is a record of the vehicle's dynamics at time  $t$ .  $x_t$  is a vector and  $x_t = [l, v]$ , where  $l$  is the location and  $v$  is the speed. In some cases, the acceleration rate,  $a$ , may also be included; that is,  $x_t = [l, v, a]$ . To model a vehicle trajectory, a specific subset of the trajectory  $\{x_t\}$ , called critical points (CPs)  $\{x_{t_i}\}$  (29), is defined as the border points of the regimes of different basic movements on the trajectory. The types of basic movements (29) include uniform motion, uniformly accelerated motion, and uniformly decelerated motion. Conversely, if the CPs are given, the trajectory of a vehicle can be reconstructed.

The overall flowchart of the proposed methodology is shown in Figure 1. CPs are first extracted from trajectories. CPs related to trivial disturbances are screened out, and five types of CPs related to the queuing process are selected for signal detection and queue length estimation. The real-time signal timing is detected, and finally, the cycle queue length is estimated. This paper is focused on a new CP extraction algorithm and a comprehensive shock wave-based queue length estimation method that is compared with the authors' previous work (29).

**Extraction of Critical Points**

A simple threshold algorithm (29) was used to identify CPs, using speed and acceleration rate. The algorithm presented here uses the location and the speed instead because not all tracking devices are able

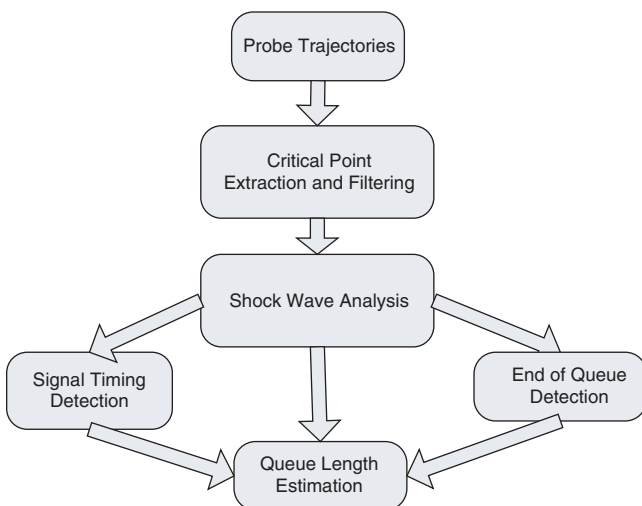


FIGURE 1 Methodology flowchart.

to provide the acceleration rate. Although it is straightforward to calculate the acceleration rate using the speed profile, the speed fluctuation caused by the measurement error is amplified by the differential calculation.

By definition, the first point on the trajectory is picked as a default CP; the problem lies in determining whether the following point indicates the same movement. If it does, this following point is not a CP; otherwise, the point is a new CP. The process restarts from the new CP until the end of the trajectory is reached.

To determine whether there is a movement change, the problem is formulated as a classification problem over an unlabeled data set. Classification has been intensively studied in the area of machine learning (31); a standard formulation procedure can be used here. The two classes are the non-CP (labeled negative) and the CP (labeled positive); trajectory points are categorized in the two classes according to a specifically defined distance to a reference point. The sample features used to classify, however, are the relative differences between consecutive points instead of the characteristics of the points themselves.

The classification algorithm is described by the following:

1. The beginning point is a natural CP and is used as the reference point.
2. The distances from other points to the beginning point is calculated as

$$dis = \sqrt{loc\_err^2 + (speed\_errT)^2} \tag{1}$$

where

loc\_err = location projection error,  
 $T$  = time interval between two continuous points, and  
 speed\_err = speed projection error.

The location projection error for the  $i$ th ( $i \geq 2$ ) point is defined as (assume the index of the beginning point is one)

$$loc\_err(i) = loc(i) - T \sum_{p=1}^{i-1} s(p) \tag{2}$$

where  $loc(i)$  is the location of the  $i$ th point and  $s(p)$  is the speed of  $p$  the point.

The speed projection error for the  $i$ th ( $i \geq 2$ ) point is defined as (assume the index of the beginning point is one)

$$speed\_err(i) = \frac{1}{i-1} \sum_{p=1}^{i-1} d(p) \tag{3}$$

where  $d(p)$  is the distance from the  $p$ th point to the line that connects the beginning point and the  $i$ th point on the time-speed space.

The line on the time-speed ( $x - y$ ) space from the beginning point to the  $i$ th point is given by

$$(y_0 - y_i)x - (x_0 - x_i)y + (x_0y_i - x_iy_0) = 0 \tag{4}$$

The speed error of point  $(x, y)$  to this line is defined as the prediction error:

$$d_i(x, y) = \left| \frac{(y_0 - y_i)x - (x_0 - x_i)y + (x_0y_i - x_iy_0)}{x_0 - x_i} \right| \tag{5}$$

3. Assume that the first  $n$  (in this study,  $n = 5$ ) points after the beginning point are in the same movement regime, named the negative pool. The mean  $\mu$  and variance  $\sigma^2$  of the distances for the points in the group can be easily calculated. For the points after the first  $n$ , the following procedure is conducted:

- a. Conduct a one-tail  $t$ -test at  $\alpha\%$  confidence level ( $\alpha = 90$  in this study) to check the hypothesis that the new point does not have significantly longer distance than the points in the pool.
  - b. If the  $t$ -test hypothesis is accepted, the point is classified as negative; add it to the negative pool and update mean  $\mu$  and variance  $\sigma^2$  using the new negative pool. If the  $t$ -test hypothesis is rejected, check the next three points. If the  $t$ -test of two or more points from the three points is rejected, a new CP has been found; update the beginning point as the new CP and go to Step 1. Otherwise, add the point to the negative pool and go to Step 3a.
4. Search until all points are checked.

In summary, this algorithm calculates the distances (Equation 1) from the following points to the beginning point, which is used as the benchmark, and uses a one-tail  $t$ -test to classify. After a new CP has been found, the beginning point is updated as the new CP until the last available point is reached. By adopting a statistic test, this algorithm is more tolerant to data noise; it also avoids subjective judgment in determination of the thresholds in the threshold algorithm as compared with the previous method (29).

### Critical Points Related to Queuing Process

The problem is to identify the CPs that are related to the queue formation and dissipation. CPs are related to changes in traffic conditions, either significant or trivial. CPs resulting from local disturbances in traffic flow should be neglected.

Figure 2 shows three shock waves and five types of CPs referred to in the following discussion. Shock Wave 1 is the queue formation shock wave; Shock Wave 2 is the queue discharging shock wave;

Shock Wave 3 is the forward propagating shock wave generated after Shock Wave 1 and Shock Wave 2 intersect. A Type I CP is the beginning point of deceleration caused by the signal light turning red. A Type II CP is the point at which the vehicle stops and joins the queue. A Type III CP is the beginning point of acceleration caused by the signal light turning green. A Type IV CP is the CP at which the arriving vehicle is slowed by the discharging queue. A Quasi-Type IV CP is a point on the trajectory at which the undelayed probe vehicle crosses the stop line. The Quasi-Type IV CP indicates the bound of time for a Type IV CP. The virtual shock wave (the bound of Shock Wave 3), which is parallel to Shock Wave 3, provides the upper bound of the queue length.

In this study, a rule-based CP filtering algorithm is used to screen out negligible CPs on the basis of time and speed characteristics. All the probe trajectories are first classified as stopped, slowed, and undelayed according to their speed profiles. Type I, II, and III CPs are from stopped trajectories, and they are selected using the method introduced in the authors' previous work (29). Type IV CPs are from slowed trajectories. A Type IV CP is the CP with minimal speed, and the time differences from the previous and next CPs are longer than 3 s. A Quasi-Type IV CP is the intersecting point of the undelayed trajectory and the stop line.

### Signal Timing Detection

Signal timing is the major factor influencing travel time on signalized arterials. Most studies related to arterial travel times use signal timing as input for the models (32–35). However, real-time signal timing is not always available for online or even offline operations. According to the 2007 National Traffic Signal Report Card (36), traffic monitoring and data collection received a grade of F, and “almost half of the agencies (43%) reported having little to no regular, ongoing program for collecting and analyzing traffic data for signal timing.” Ban et al. explored a method to derive signal timing using the delay measurements by virtual trip line technology based

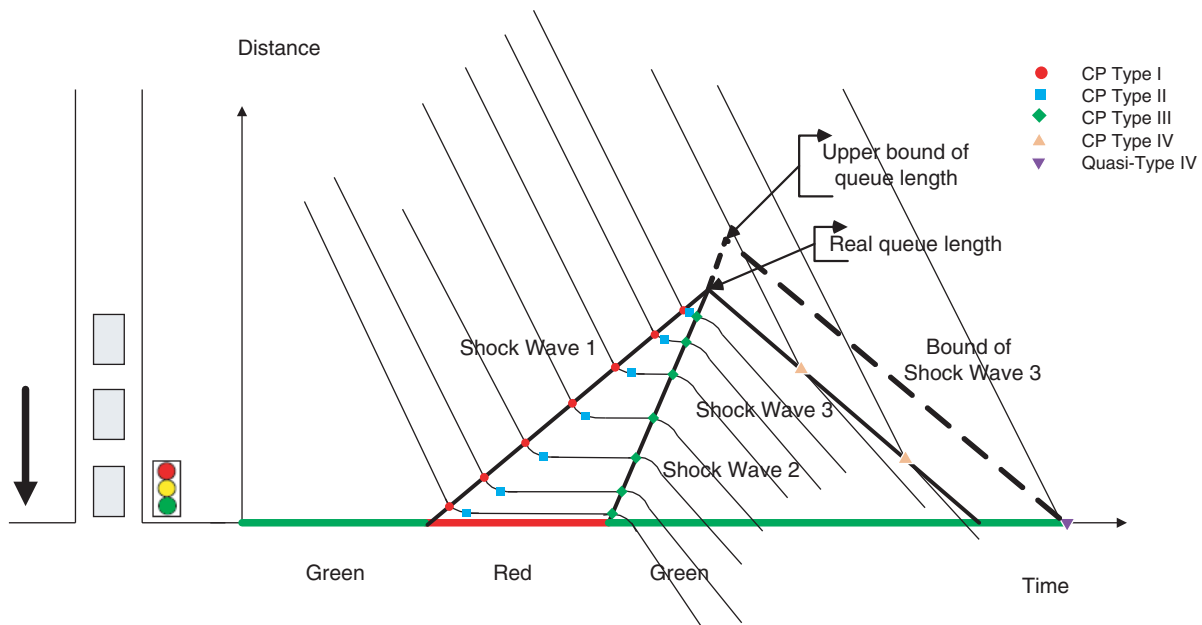


FIGURE 2 Circutinal points related to queue.

on GPS-equipped cell phones (37). Using sampled travel times, they found that a 40% penetration rate of the probe was needed to obtain reliable signal timing detection. A shock wave method (29) was used for real-time signal timing detection; the method detects signal timing information with a lower sample rate.

The shock wave speeds are calculated with the Lighthill–Whitham–Richards model (38–40). Only the final equations are listed in this paper. Details are available in the authors' previous work (29).

The start time of the green light can be calculated as

$$T_g = T_{CP\ III} - \frac{L_{CP\ III}}{q_s} (k_j - k_m) \quad (6)$$

where

$$\begin{aligned} T_{CP\ III} &= \text{time stamp of the Type III CP,} \\ L_{CP\ III} &= \text{distance from the Type III CP to the stop bar,} \\ q_s &= \text{saturation flow rate,} \\ k_m &= \text{saturation flow density, and} \\ k_j &= \text{jam density.} \end{aligned}$$

The start time of the red light can be obtained by

$$T_r = T_{CP\ I} - \frac{L_{CP\ I}}{v_{CP\ I}} (L_{CP\ I} / L_{CP\ II} - 1) \quad (7)$$

where

$$\begin{aligned} T_{CP\ I} &= \text{time stamp of the Type I CP,} \\ L_{CP\ I} &= \text{distance from the Type I CP to the stop bar,} \\ L_{CP\ II} &= \text{distance from the Type II CP to the stop bar, and} \\ v_{CP\ I} &= \text{speed of the Type I CP.} \end{aligned}$$

### Dynamic Queue Length Estimation

The definition of queue length differs among studies. Some studies use the number of vehicles, whereas some use the distance. Occasionally, only stopped vehicles are considered to be in the queue; in other cases, the slowly moving vehicles arriving at the rear of the queue are also counted. In this study, the queue length is defined as the distance from the front bumper of the last stopped or slowly moving (less than 5 mph) vehicle to the stop bar before the intersection.

The queue length estimation model consists of two submodels: one based on the instantaneous queue length and one based on Shock Wave 3. The instantaneous queue length is defined as the queue length at a specific time stamp when the queue is cumulating. From the foregoing analysis, the available Type II CPs indicate the profile of the instantaneous queue length. The instantaneous queue length submodel (29) depends on Type II CPs to estimate the arrival rate to obtain the queue length estimation. Because the progress of queue formation is greatly affected by the arrival pattern, different arrival assumptions are made according to intersection control types. This submodel is summarized as follows.

#### Estimation Based on Instantaneous Queue Length

An isolated intersection's arrival traffic is not affected by the upstream signalized intersection. The *Highway Capacity Manual* defines an isolated intersection as "at least 1 mile from the nearest upstream signalized intersection" (41). For an isolated intersection,

the arrival flow rate within a cycle can be assumed to be constant. Therefore, the queue length increases at a constant rate and can be easily calculated using the detected instantaneous queue length. Given the already detected signal timing, the maximum queue length can be calculated as

$$L_q = \frac{q_s q_u (T_g - T_r)}{k_j (q_s - q_u)} \quad (8)$$

where

$$\begin{aligned} q_u &= \text{upstream arrival flow rate,} \\ q_s &= \text{saturation flow rate,} \\ T_g, T_r &= \text{start time of green and red lights (Figure 2), respectively,} \\ &\text{and} \\ k_j &= \text{jam density.} \end{aligned}$$

The upstream arrival rate  $q_u$  can be estimated as

$$q_u = \frac{L_{CP\ II} k_j}{T_{CP\ II} - T_r} \quad (9)$$

where  $L_{CP\ II}$  is the distance from the Type II CP to the stop bar and  $T_{CP\ II}$  is the time stamp of the Type II CP.

For an intersection affected by an upstream signal, the arrival pattern varies significantly within a cycle. As an approximation, the queue increase process is modeled as a piecewise linear line. More than one Type II CP is needed for this case. Assume there are  $n - 1$  available Type II CPs, and use the point at the start of red as the additional point (the distance to the stop bar is zero); order them chronologically as a list of points on the queue length and time plane. The average queue increase rate between each two consecutive points can be calculated as

$$q_i = \frac{L_{CP\ II, i+1} - L_{CP\ II, i}}{T_{CP\ II, i+1} - T_{CP\ II, i}} \quad (10)$$

where

$$\begin{aligned} i &= \text{index, } i = 0, 2, \dots, n - 2, \\ L_{CP\ II, i} &= \text{distance from the } i\text{th Type II CP to the stop bar, and} \\ T_{CP\ II, i} &= \text{time stamp of the } i\text{th Type II CP.} \end{aligned}$$

Then several queue length estimates can be obtained:

$$\begin{aligned} L_{\max} &= L_{CP\ II, n} + q_{\max} t_{g, n} \\ L_{\text{last}} &= L_{CP\ II, n} + q_{n-1} t_{g, n} \\ L_{\min} &= L_{CP\ II, n} \end{aligned} \quad (11)$$

where

$$\begin{aligned} L_{\max}, L_{\text{last}}, L_{\min} &= \text{three queue length estimates, which use the maximum queue increase rate, the last available queue increase rate, and no queue increase, respectively;} \\ q_{\max} &= \text{maximum of all the } q_i; \text{ and} \\ t_{g, n} &= \text{time from the last Type II CP to line of Shock Wave 2; it is calculated by} \end{aligned}$$

$$t_{g, n} = \frac{L_{CP\ II, n}}{v_2} + T_g - T_{CP\ II, n} \quad (12)$$

on the basis of the line equation of Shock Wave 2 ( $y = v_2(x - t_g)$ ), where  $v_2$  is the speed of Shock Wave 2.

The queue length of the cycle is therefore estimated as a weighted average:

$$L_q = w_1 L_{\max} + w_2 L_{\text{last}} + w_3 L_{\min} \quad (13)$$

where  $w_1, w_2, w_3$  are the weights and  $w_1 + w_2 + w_3 = 1$ ,  $w_1, w_2, w_3 \geq 0$ . In this study,

$$w_2 = w_3 = \frac{t_{g, \max}}{2t_{g, \max} + t_{g, n}}$$

and

$$w_1 = \frac{t_{g, n}}{2t_{g, \max} + t_{g, n}}$$

where  $t_{g, \max}$  is the time from the latter Type II CP on the segment where the maximum queue increase rate is achieved. The farther from Shock Wave 2, the smaller the weight.

### Estimation Based on Shock Wave 3

It is intuitive that because the movement of a vehicle is determined almost entirely by the vehicle before it, only the traffic information before the probe vehicle can be obtained. Therefore, in using the stopped probe vehicles (as the instantaneous queue length submodel), only the lower bound of the queue length is guaranteed. However, Shock Wave 3 is generated after the queue reaches its maximum length, and therefore, CPs related to Shock Wave 3 (Type IV and Quasi-Type IV) are able to provide additional information about the queue length.

The speed of Shock Wave 3 is calculated by Equation 14:

$$v_3 = \frac{q_s - q_u}{k_s - k_u} \quad (14)$$

where

$$\begin{aligned} q_s &= \text{saturation flow rate,} \\ q_u &= \text{upstream arrival flow rate,} \\ k_s &= \text{saturation flow density, and} \\ k_u &= \text{upstream density.} \end{aligned}$$

Assuming the time axis is the  $x$ -axis and the distance to the stop bar is the  $y$ -axis (as shown in Figure 2), Shock Wave 2 and Shock Wave 3 are described by Equations 15 and 16, respectively:

$$y = v_2(x - T_g) \quad (15)$$

$$y = -v_3(x - T_{\text{CP IV}}) + L_{\text{CP IV}} \quad (16)$$

where  $T_{\text{CP IV}}$  is the time of the Type IV CP and  $L_{\text{CP IV}}$  is the distance from the Type IV CP to the stop bar.

The intersection point of the two lines is represented as

$$\begin{cases} x = \frac{v_2 T_g + v_3 T_{\text{CP IV}} + L_{\text{CP IV}}}{v_2 + v_3} \\ y = \frac{v_2 v_3 (T_{\text{CP IV}} - T_g) + v_2 L_{\text{CP IV}}}{v_2 + v_3} \end{cases} \quad (17)$$

The value of the  $y$ -coordinate is the queue length.

It is intuitive that the portion of the Type IV CP is much smaller than Type I, II, or III because Shock Wave 3's forward propagation

results in a much narrower time window for Type IV CPs (Figure 2). In fact, the undelayed probe vehicles could also provide information about the queue length. As shown in Figure 2, a Quasi-Type IV CP is defined when an undelayed probe vehicle transverses the stop line. Therefore, the virtual shock wave (the bound of Shock Wave 3) provides an estimate of the upper bound of the queue length.

This virtual shock wave is described by Equation 18:

$$y = -v_3(x - T_{\text{Q,IV}}) \quad (18)$$

where  $T_{\text{Q,IV}}$  is the time of the Quasi-Type IV CP.

The intersection point of the two lines ( $y$  is the queue length) is

$$\begin{cases} x = \frac{v_2 T_g + v_3 T_{\text{Q,IV}}}{v_2 + v_3} \\ y = \frac{v_2 v_3 (T_{\text{Q,IV}} - T_g)}{v_2 + v_3} \end{cases} \quad (19)$$

The problem here is how to estimate the speed of Shock Wave 3,  $v_3$ . If more than one Type IV CP is available, the speed of Shock Wave 3 can be readily calculated. For cases in which only one Type IV CP is available, the upper bound of the queue length can be obtained using the possible range of the speed of Shock Wave 3, which can be estimated according to the fundamental diagram in Figure 3.

The shock wave speed equals the slope of the line connecting the two traffic flow states. Whether the shock wave is forward or backward propagating is determined by whether the slope is positive or negative. Although different fundamental diagrams have different shapes, the density–flow functions before saturation are nonconvex. That is, the upstream arrival flow rate  $q_u$  is less than saturation flow rate  $q_s$ ; the upstream vehicle speed  $v_u$  is higher than the saturation flow speed  $v_s$ ; and the upstream density  $k_u$  is less than saturation density  $k_s$ . Therefore, the shock wave speed is between 0 and  $v_s$ . The upper bound of the queue lengths can be obtained accordingly.

Furthermore, the results of the two submodels could be combined. Table 1 shows how to combine the estimates for different CP availability scenarios.

## DATA SOURCE

Three data sets were used in this study: a simulation data set, an NGSIM (42) data set, and a GPS data set collected in a recent field study.

The simulation data set was generated by a hypothetical arterial corridor network built in Paramics microsimulation software. The speed limit on the corridor is 40 mph and the cycle lengths of the intersection signals are 80 s with 45 s green time. Signals are coordinated, and the offsets of signals are equal to the free-flow travel times. As shown in Table 2, the data from a boundary intersection were used in the isolated intersection scenario, and the data from a middle intersection were used in the nonisolated intersection case. Two levels of demand were used for different traffic flow conditions: 800 vehicles per hour per lane for the off-peak hour and 1,800 vehicles per hour per lane for the peak hour.

The Peachtree data set from the NGSIM (42) was chosen in this study. This data set was obtained from a 2,100-ft segment of Peachtree Street in Atlanta, Georgia, collected between 4:00 and 4:15 p.m. November 8, 2006. This street is a north–south street with a speed limit of 35 mph. Trajectory data were collected by

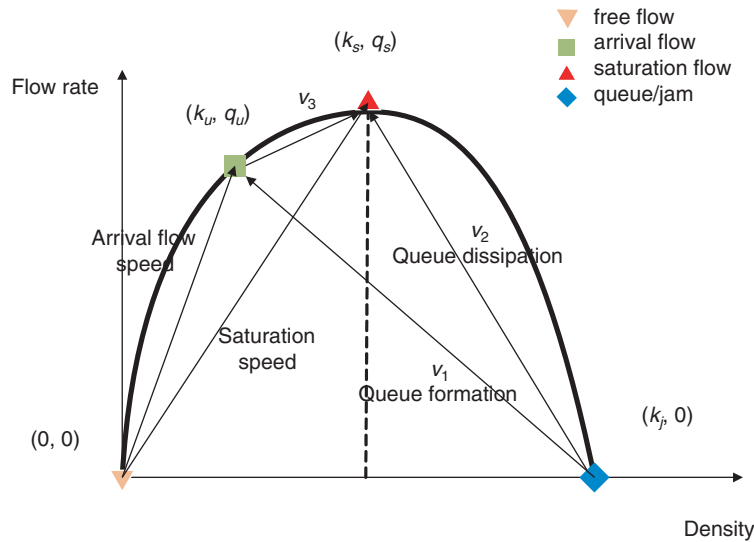


FIGURE 3 Traffic states on fundamental diagram.

video cameras mounted on a 30-story roadside building. Intersections on the segment were coordinated with a cycle length of 100 s during the collection time.

The GPS log data set was collected in Brookings, South Dakota, April 7, 2010. A section of US-14 (also called 6th Street) was

TABLE 1 CP Scenarios and Result Fusion

	Type II CP	
	Available	Unavailable <sup>a</sup>
Type IV and Quasi-Type IV	Available	Unavailable <sup>a</sup>
Quasi-Type IV	Weighted average <sup>b</sup> of the results of Equation 8 (isolated intersection) or Equation 13 (nonisolated intersection) and Equation 19.	Equation 19
One Type IV CP	Weighted average <sup>a</sup> of the results of Equation 8 (isolated intersection) or Equation 13 (nonisolated intersection) and Equation 17.	Equation 17
Two Type IV or more	Average of the results of Equation 8 (isolated intersection) or Equation 13 (nonisolated intersection) and Equation 17.	Equation 17
Unavailable	Equation 8 (isolated intersection) or Equation 13 (nonisolated intersection)	Use the previous cycle's estimate

<sup>a</sup>When Type II CP is not available, signal timing cannot be obtained because Type I and III CPs are not available either.  $T_g$  in the equation is calculated using the signal parameters of the previous cycle.

<sup>b</sup>The weights are calculated as

$$w_1 = \frac{l_2}{l_1 + l_2}$$

$$w_2 = 1 - w_1$$

where  $l_1, l_2$  are time distances from the Type II and Type IV–Quasi-Type IV CPs to Shock Wave 2.

chosen as the test bed (shown in Figure 4). US-14 is a major east–west corridor carrying the largest traffic volume of any roadway in Brookings. The posted speed limit is 35 mph. The data collection was from 4:15 to 5:30 p.m., which covered the peak hour. The intersection peak-hour traffic volumes vary from 2,800 to 3,500 at these intersections. Twelve probe vehicles were used. The GPS data logger recorded second-by-second position and speed data, with a position accuracy of 3 m root mean square error with differential GPS and a speed accuracy of 0.12 mph root mean square. (Differential GPS is an enhancement to GPS that uses a network of fixed, ground-based reference stations to alleviate handset measurement errors.) Four video cameras were mounted to record the actual signal timing parameters and queue lengths for each cycle.

### NUMERICAL EXPERIMENT RESULTS

The performance of the queue length estimation is measured by mean absolute percentage error (MAPE):

$$MAPE = \frac{1}{n} \sum_{i=1}^n \left| \frac{\text{groundtruth} - \text{estimation}}{\text{groundtruth}} \right| \times 100\% \quad (20)$$

where  $n$  is the total trial number and groundtruth is the actual queue length being estimated.

TABLE 2 Simulation Data Sets

Scenario	Source
Isolated intersection, off-peak	Upstream link of a boundary intersection
Isolated intersection, peak	
Nonisolated intersection, off-peak	Middle intersection affected by upstream signal
Nonisolated intersection, off-peak	

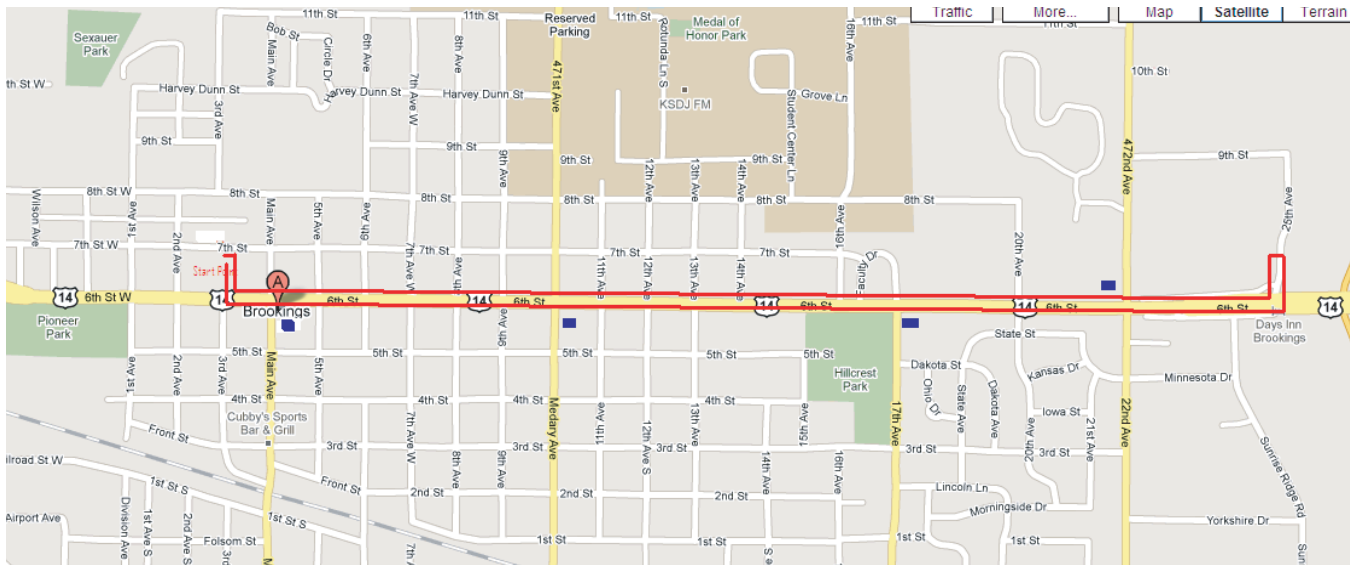


FIGURE 4 Field data collection route (red lines indicate route of probe vehicles; blue squares show study intersection).

For the isolated intersection case, one trajectory was randomly picked for estimation in each cycle. For the coordinated intersection cases, three trajectories were randomly picked in each cycle. For each case, experiments were run 20 times. For the GPS log data set, to obtain the ground truth queue length, the number of vehicles in the queue was recorded and multiplied by the average distance headway.

Table 3 summarizes the experiment results.

For the GPS log data set, the eastbound approach on 22nd Avenue is used as the case study. The MAPE of the queue length estimation is 25.49% within the 12 recorded cycles. One cause for a higher MAPE than that obtained for the first two data sets is that the ground truth queue length was calculated by the number of queued vehicles simply multiplied by the predefined distance headway (25 ft). In addition, engineering judgment was applied to determine whether a vehicle was in the queue.

The MAPE for all the scenarios of validation and evaluation is around 20%, a promising outcome. Depending on the data set used, the model would have larger errors (overestimates) in two special cases: (a) when the arrival rate changes greatly within a cycle (in some cycles of the NGSIM data set, the traffic changes from the saturation flow to almost zero) and only Type II CPs are available; and (b) when the queue length is quite short and only Quasi-Type IV CPs are available.

This phenomenon can be explained in two ways: (a) for the estimation based on instantaneous queue length (using Type II CPs), a higher flow rate leads to a higher probability to have a picked trajectory (the probe vehicle), which leads to a higher detected arrival rate and therefore, an overestimated queue length; (b) because the Shock Wave 3 submethod (using Quasi-Type IV CPs) calculates the upper bound of the queue length despite the real queue length, the shorter the queue, the larger the error. However, without the occurrences of the two special cases, the performance of this method would be much better.

### CONCLUSION AND FUTURE WORK

An improved approach for estimating queue length with vehicle trajectory data is proposed. To address the challenge of converting the microscopic detections into macroscopic performance measurements, a CP extraction method is presented. CPs on vehicle trajectories are defined as the points representing the changing vehicle dynamics. This CP extraction algorithm also has the potential to reduce communication costs for probe vehicles in real-time data collection applications. To identify queue formation and dissipation shock waves, five types of special CPs related to the queuing process are then defined and chosen from the extracted CPs. Through the application of Lighthill–Whitham–Richards shock wave theory, an improved queue length estimation method based on shock waves is proposed. The model can provide cycle-by-cycle queue length estimation and is evaluated by three data sets: a simulated data set, an NGSIM data set, and a field-collected GPS data set. The results indicate that this trajectory-based approach is promising. Two special cases that may cause larger errors of the queue estimation are also discussed.

This method can provide travelers with instantaneous arterial traffic conditions in real-time applications. If only offline trajectory data are available, this method can still be implemented in the evaluation and optimization of arterial traffic control systems. It could also be applied in the IntelliDrive environment when integrated into the roadside or intersection infrastructures. A future study includes improvement in the model to reduce overestimation in the two special cases through the use of additional data, such as the queue length estimates of previous cycles or upstream intersections.

TABLE 3 MAPE of Queue Length (in Distance) Estimation

Signal Setting	Data Set	Scenarios and Intersection	No. of Cycles	MAPE (%)
Isolated	Simulation	Nonpeak	12	17.46
		Peak	12	19.23
Coordinated	Simulation	Nonpeak	12	20.61
		Peak	12	21.57
		At 10th (SB)	7	20.92
	GPS log	At 11th (SB)	7	19.11
		At 12th (SB)	7	21.72
		At 13th (SB)	7	22.26
	At 22nd (EB)	12	25.49	

NOTE: SB = southbound; EB = eastbound.

## REFERENCES

- Hendren, P. G., L. A. Neumann, and S. M. Pickrell. Linking Performance-Based Program Development and Delivery. In *Conference Proceedings 36: Performance Measures to Improve Transportation Systems: Summary of the Second National Conference*, Transportation Research Board of the National Academies, Washington, D.C., 2006, pp. 121–130.
- Webster, F. V. Traffic Signal Settings. Road Research Technical Paper 39. Road Research Laboratory, Her Majesty's Stationery Office, London, England, 1958.
- Sharma, A., D. M. Bullock, and J. A. Bonneson. Input–Output and Hybrid Techniques for Real-Time Prediction of Delay and Maximum Queue Length at Signalized Intersections. In *Transportation Research Record: Journal of the Transportation Research Board, No. 2035*, Transportation Research Board of the National Academies, Washington, D.C., 2007, pp. 69–80.
- Akcelik, R. *A Queue Model for HCM 2000*. ARRB Transportation Research Ltd., Melbourne, Victoria, Australia, 1999.
- May, A. D. *Traffic Flow Fundamentals*. Prentice Hall, Englewood Cliffs, N.J., 1990.
- Michalopoulos, P. G., G. Stephanopoulos, and V. B. Pisharody. Modeling of Traffic Flow at Signalized Links. *Transportation Science*, Vol. 14, No. 1, 1980, pp. 9–41.
- Stephanopoulos, G., P. G. Michalopoulos, and G. Stephanopoulos. Modelling and Analysis of Traffic Queue Dynamics at Signalized Intersections. *Transportation Research Part A*, Vol. 13, No. 5, 1979, pp. 295–307.
- Skabardonis, A., and N. Geroliminis. Real-Time Monitoring and Control on Signalized Arterials. *Journal of Intelligent Transportation Systems*, Vol. 12, No. 2, 2008, pp. 64–74.
- Liu, H. X., X. Wu, W. Ma, and H. Hu. Real-Time Queue Length Estimation for Congested Signalized Intersections. *Transportation Research Part C*, Vol. 17, No. 4, 2009, pp. 412–427.
- Miller, A. J. *Signalised Intersections—Capacity Guide*. Bulletin 4. Australian Road Research Board, Melbourne, Victoria, 1968.
- Robertson, D. I. *TRANSYT: A Traffic Network Study Tool*. Transport Research Laboratory, Berkshire, England.
- Rouphail, N. M., K. G. Courage, and D. W. Strong. New Calculation Method for Existing and Extended *Highway Capacity Manual* Delay Estimation Procedures. Presented at 85th Annual Meeting of the Transportation Research Board, Washington, D.C., 2006.
- Strong, D. W., and N. M. Rouphail. Incorporating Effects of Traffic Signal Progression into Proposed Incremental Queue Accumulation Method. Presented at 85th Annual Meeting of the Transportation Research Board, Washington, D.C., 2006.
- Akcelik, R. The Highway Capacity Manual Delay Formula for Signalized Intersections. *ITE Journal*, Vol. 58, No. 3, 1988, pp. 23–27.
- Geroliminis, N., and A. Skabardonis. Prediction of Arrival Profiles and Queue Lengths Along Signalized Arterials by Using a Markov Decision Process. In *Transportation Research Record: Journal of the Transportation Research Board, No. 1934*, Transportation Research Board of the National Academies, Washington, D.C., 2005, pp. 116–124.
- Viti, F. *The Dynamics and the Uncertainty of Delays at Signals*. PhD dissertation. TRAIL Research School, Delft University of Technology, Netherlands, 2006.
- Viti, F., and H. J. van Zuylen. Modeling Queues at Signalized Intersections. In *Transportation Research Record: Journal of the Transportation Research Board, No. 1883*, Transportation Research Board of the National Academies, Washington, D.C., 2004, pp. 68–77.
- Wang, H., K. Rudy, and D. Ni. Modeling and Optimization of Link Traffic Flow. Presented at 87th Annual Meeting of the Transportation Research Board, Washington, D.C., 2008.
- Michalopoulos, P. G., G. Stephanopoulos, and G. Stephanopoulos. An Application of Shock Wave Theory to Traffic Signal Control. *Transportation Research Part B*, Vol. 15, No. 1, 1981, pp. 35–51.
- Ban, X., and P. Hao. Real-Time Queue Length Estimation for Signalized Intersections Using Sampled Travel Times. Presented at 89th Annual Meeting of the Transportation Research Board, Washington, D.C., 2010.
- Geroliminis, N., and A. Skabardonis. Real Time Vehicle Reidentification and Performance Measures on Signalized Arterials. *Proc.*, 2006 *IEEE Intelligent Transportation Systems Conference*, Toronto, Canada, Sept. 17–20, 2006, pp. 188–193.
- Lu, X.-Y., and A. Skabardonis. Freeway Traffic Shockwave Analysis: Exploring NGSIM Trajectory Data. Presented at 86th Annual Meeting of the Transportation Research Board, Washington, D.C., 2007.
- Izadpanah, P., B. Hellinga, and L. Fu. Automatic Traffic Shockwave Identification Using Vehicles' Trajectories. Presented at 88th Annual Meeting of the Transportation Research Board, Washington, D.C., 2009.
- Comert, G., and M. Cetin. Queue Length Estimation from Probe Vehicle Location: Undersaturated Conditions. Presented at 86th Annual Meeting of the Transportation Research Board, Washington, D.C., 2007.
- Shladover, S. E., and T. M. Kuhn. Traffic Probe Data Processing for Full-Scale Deployment of Vehicle–Infrastructure Integration. In *Transportation Research Record: Journal of the Transportation Research Board, No. 2086*, Transportation Research Board of the National Academies, Washington D.C., 2008, pp. 115–123.
- Claudel, C. G., A. Hofleitner, N. Mignerey, and A. M. Bayen. Guaranteed Bounds on Highway Travel Times Using Probe and Fixed Data. Presented at 88th Annual Meeting of the Transportation Research Board, Washington, D.C., 2009.
- Daganzo, C. F. A Variational Formulation of Kinematic Waves: Basic Theory and Complex Boundary Conditions. *Transportation Research Part B*, Vol. 39, No. 2, 2005, pp. 187–196.
- Newell, G. F. A Simplified Theory of Kinematic Waves in Highway Traffic, Part I: General Theory. *Transportation Research Part B*, Vol. 27, No. 4, 1993, pp. 281–287.
- Cheng, Y., X. Qin, J. Jin, and B. Ran. An Exploratory Shockwave Approach for Signalized Intersection Performance Measurements Using Probe Trajectories. Presented at 89th Annual Meeting of the Transportation Research Board, Washington, D.C., 2010.
- FHWA, U.S. Department of Transportation. Next generation simulation website. <http://www.ngsim.fhwa.dot.gov/>. Accessed May 6, 2009.
- Mitchell, T. *Machine Learning*. McGraw-Hill, New York, 1997.
- Levinson, D. M. Speed and Delay on Signalized Arterials. *ASCE Journal of Transportation Engineering*, Vol. 124, No. 3, 1998, pp. 258–263.
- Zhang, H. M. Link–Journey–Speed Model for Arterial Traffic. In *Transportation Research Record: Journal of the Transportation Research Board, No. 1676*, TRB, National Research Council, Washington D.C., 1999, pp. 109–115.
- Chen, M., and S. I. J. Chien. Determining the Number of Probe Vehicles for Freeway Travel Time Estimation by Microscopic Simulation. In *Transportation Research Record: Journal of the Transportation Research Board, No. 1719*, Transportation Research Board of the National Academies, Washington D.C., 2000, pp. 61–68.
- Xie, C., R. L. Cheu, and D.-H. Lee. Calibration-Free Arterial Link Speed Estimation Model Using Loop Data. *ASCE Journal of Transportation Engineering*, Vol. 127, No. 6, 2001, pp. 507–514.
- 2007 National Traffic Signal Report Card: Technical Report. National Transportation Operations Coalition, Washington, D.C., 2007.
- Ban, X., R. Herring, P. Hao, and A. M. Bayen. Delay Pattern Estimation for Signalized Intersections Using Sampled Travel Times. In *Transportation Research Record: Journal of the Transportation Research Board, No. 2130*, Transportation Research Board of the National Academies, Washington D.C., 2009, pp. 109–119.
- Lighthill, M. J., and G. B. Whitham. On Kinematic Waves. I. Flood Movement in Long Rivers. *Proceedings of the Royal Society of London: Series A, Mathematical and Physical Sciences*, Vol. 229, No. 1178, 1955, pp. 281–316.
- Lighthill, M. J., and G. B. Whitham. On Kinematic Waves. II. A Theory of Traffic Flow on Long Crowded Roads. *Proceedings of the Royal Society of London: Series A, Mathematical and Physical Sciences*, Vol. 229, No. 1178, 1955, pp. 317–345.
- Richards, P. I. Shock Waves on the Highway. *Operations Research*, Vol. 4, No. 1, 1956, pp. 42–51.
- Highway Capacity Manual*. TRB, National Research Council, Washington, D.C., 2000.
- Alexiadis, V., J. Colyar, and J. Halkias. The Next Generation Simulation Program. *ITE Journal*, Vol. 74, No. 8, 2004, pp. 22–26.